Conf-820306--4

Lifetime improvement of sheathed thermocouples for use in high-temperature and thermal transient operations[a]

R. W. McCulloch[b]

Oak Ridge National Laboratory, Oak Ridge, Tennessee 37830

J. H. Clift[c]

Y-12 Development Division, Oak Ridge, Tennessee 37830

CONF-820306--4

DE82 008844

ABSTRACT

Premature failure of small-diameter, magnesium-oxide-insulated sheathed thermocouples occurred when they were placed within nuclear fuel rod simulators (FRSs) to measure high temperatures and to follow severe thermal transients encountered during simulation of nuclear reactor accidents in Oak Ridge National Laboratory (ORNL) thermal-hydraulic test facilities. Investigation of thermally cycled thermocouples yielded three criteria for improvement of thermocouple lifetime: (1) reduction of oxygen impurities prior to and during their fabrication, (2) refinement of thermoelement grain size during their fabrication, and (3) elimination of prestrain prior to use above their recrystallization temperature. The first and third criteria were satisfied by improved techniques of thermocouple assembly and by a recovery anneal prior to thermocouple use.

Grain-size refinement to ASTM *macrograin* size 9 (3970 grains/mm^2) was accomplished by adopting an appropriate annealing schedule and optimizing the drawing process. The general drawing equation was extended to describe thermocouple internal stresses, process parameters were evaluated and optimized, and a multiple-pass draw schedule was developed that increased cold work (true strain) between anneals from 25 to 55%. Maximum first-draw cold work was limited to ~42% by frictional work that was found to be 25% higher for thermocouple drawing than for equivalent wire drawing. Second-draw cold work was limited to 10 to 20% by friction and high yield stress. More than 3500 m of refined grain material was produced; longest average lengths of ~100 m were obtained with a single-draw process of 40% cold work between anneals.

SUBJECT INDEX

1. Type K thermocouples - sheathed.
2. Type K thermocouples - fabrication.
3. Transient behavior of thermocouples.

---

[a]Research sponsored by the Office of Research and Technology, U.S. Department of Energy under contract W-7405-eng-26 with the Union Carbide Corporation-Nuclear Division.

INTRODUCTION

Small-diameter sheathed thermocouples are the principal means of temperature measurement in large out-of-reactor thermal-hydraulic test facilities at ORNL and other national laboratories, as well as at several private companies conducting reactor safety experiments. High temperatures (up to 1200°C) as well as temperature transients (up to 50°C/s) are often required. The reliability of 0.51-mm, sheathed, insulated-junction type K thermocouples used in these experiments has improved significantly in the last few years and, in general, has met program needs. However, requirements for small-diameter thermocouples for use in the developing Gas-Cooled Fast Breeder Reactor-Core Flow Test Loop (GCFR-CFTL) program at ORNL necessitated a marked increase in reliability for the CFTL to meet successfully its objectives.

CFTL FRS DESCRIPTION

The CFTL (Fig. 1) is a high-temperature, high-pressure, fast-transient, out-of-reactor gas loop that was designed to supply helium to a test bundle at appropriate temperature and pressure conditions. The test bundle consists of electrically heated FRSs that are arranged to represent a segment of the GCFR core. The CFTL is designed to accommodate rod bundles of 37 to 91 FRSs and to operate from ambient pressure to 10.3 MPa, from 300 to 1370°C, and at FRS power levels from 0 to 43 kW/rod (0 to 4 MW total power). The principal objectives of the test program were the acquisition and analysis of test data on (1) thermal and pressure-drop characteristics, (2) design and safety margins, and (3) friction and thermal mechanical behavior of test bundles that simulate portions of GCFR fuel and control assemblies during steady-state or transient operation. Transient operation included prescribed variations (with time) of test bundle power, helium pressure, and coolant flow rate to simulate normal, upset, emergency, and faulted accident transients. Data to be obtained were primarily from the subject thermocouples, most of which are integral components of the FRSs.

The design of the CFTL FRS is shown in Fig. 2. The FRS cladding is prototypic of GCFR 316 stainless-steel-alloy fuel rod cladding and thus has the same dimensions, configuration, and thermal and mechanical characteristics. The length of the FRS is 2860 mm, 1200 mm of which is heated; the outside diameter is 8.0 mm. A length of 1220 mm of the outer surface, slightly overlapping the heated length, is roughened to enhance

heat transfer to the helium. The FRS is reentrant in design; that is, both power terminals enter at a single end. The outer terminal, a copper tube, is joined to a tubular nickel conductor that, in turn, is joined to one end of the variable-width heating element designed to provide a cosine heat-flux distribution. The center terminal is made of a solid copper rod that is joined to a nickel conductor. This conductor, in turn, is joined through an adapter to the other end of the heating element to complete the electric-current-carrying circuit in the FRS.

Six type K thermocouples (four in earlier FRSs) with insulated measuring (hot) junctions are installed inside the FRS cladding. The sheaths of the thermocouples run longitudinally along the inside surface of the clad at 60° angular intervals. Each of the six thermocouple junctions is located axially with a tolerance of ±1 mm and is required to provide temperature information over an extremely wide range. Table I summarizes these requirements. The combinations of violent thermal cycling, high temperatures, and long lifetime are severe requirements for small-diameter type K thermocouples.

INITIAL FRS QUALIFICATION TESTS

To qualify the CFTL FRS and its thermocouples, operation is at various steady-state conditions from 300 to 1100°C for 100 to 200 h, including 40 h at 1100°C. The CFTL FRS is then subjected to more than 2000 thermal cycles for a total operation time of about 1000 h. Thermal transients are normally from 1 to 50°C/s, and the temperature changes during cycling are from 150 to 600°C.

Initially, four FRSs were tested, into which a total of 13 small-diameter insulated-junction thermocouples had been installed. About 1200 h of steady-state and transient-cycling tests were conducted on the FRSs, and over 1000 thermal transients were conducted on one of them having 4 thermocouples. Most thermocouples failed in the initial steady-state portion of the tests. Those thermocouples that did survive the steady-state tests failed within a few hundred transient cycles. Failure in all cases was by development of an open circuit in one or both of the thermoelements at elevated temperatures. When the FRS temperature was lowered, the thermocouples would again become operative. Photomicrographs of failed thermocouples showed voids at the grain boundaries of both thermoelements, and both thermocouples were extremely brittle.

These negative results prompted investigation into the causes and mechanisms for failure. Investigations

were primarily directed toward lifetime improvement. Previous work by Potts and McElroy[1] and by Anderson and Kollie[2] showed that small-diameter thermocouples are susceptible to metallurgical, chemical, and mechanical changes and that these changes affect both lifetime and accuracy.

THERMOCOUPLE INVESTIGATIONS

To understand the factors that contribute to the premature failure of small-diameter thermocouples, both their physical structure and metallurgical state must be considered.

A thermocouple consists of two thermoelements, an insulating material, and a metal sheath (Fig. 2). One thermoelement is Chromel-P* (the K+ alloy), a nickel-based alloy having chromium and silicon as the major alloying elements. The other thermoelement is Alumel* (the K- alloy), a nickel-based alloy containing aluminum, manganese, silicon, and cobalt as major alloying elements. The final average grain size of both thermoelements was specified for CFTL use to be ASTM micrograin size 7 (992 grains/ mm^2) or smaller. Thermoelement wires are contained in a magnesium oxide insulation also having a particle size of ASTM micrograin size 7 or smaller. The sheath is Inconel 600,† a nickel-based alloy. The thermoelement wire diameter and the sheath thickness are 0.076 to 0.089 mm. Thus, the thermoelement grain size and wire diameter are such that as few as four to six grains traverse the entire thermoelement cross section. Grain boundaries represent material discontinuities and, at high temperatures, are relatively weak compared with the rest of the material;[3] therefore, regions along the thermoelement with large grains are weak points within the structure.

Another closely related factor influencing lifetime is thermal stress arising from differential thermal expansion between the thermocouple components and other FRS components. Figure 3 (Ref. 4) gives a comparison of the thermal expansion of the 316 stainless steel used as the FRS cladding, the Inconel 600 thermocouple sheath material, and the Chromel and Alumel thermoelement materials. At 1000°C, the 316 stainless steel clad expanded 20% more than the Chromel thermoelement and 30% more than the Alumel thermoelement. The thermocouple is intimately associated with the much more massive FRS clad, and both thermoelements are put

*Trade name of the Hoskins Manufacturing Company.
†Trade name of the International Nickel Company.

into tension as temperatures are increased. These tensile forces, imposed on grains only slightly smaller than the thermoelement lead wires, are major contributors to premature thermocouple failure.

A third contributing factor is that of oxidation. Spooner and Thomas,[5] operating bare Chromel and Alumel wires in various environments, found that oxidation of both Chromel and Alumel thermoelements resulted in embrittlement and early failure, especially when the thermocouples were operated in the temperature range of 81° to 1038°C.

A final factor that has been found to make thermocouples susceptible to both early failure and temperature measurement errors is residual cold work, or prestrain, in the thermoelements prior to their use at temperatures above their recrystallization temperature.

Potts and McElroy[1] have shown the importance of a fully recrystallized microstructure, free of material cold work, as the final fabrication step for type K thermoelements. Cold working changes the Seebeck coefficient of the material, and, during use in an FRS, the cold worked material will be annealed, again changing the Seebeck coefficient. Changes in the Seebeck coefficient of a thermocouple cause temperature measurement errors.

In addition to causing errors, small amounts of cold work have been shown to cause relatively large increases in grain size, possibly by a factor of 2 or 3 (Ref. 6), when a material recrystallizes. Figure 4 illustrates the effect of cold work on recrystallized grain size. With thermoelement grain diameter already not much smaller than the wire diameter, low levels of prestrain clearly should be avoided, if only to preserve a small grain size following recrystallization.

Anderson[7] conducted tests to determine the combined effects of grain size, prestrain, and differential thermal expansion on thermocouple lifetime. Thermocouple specimens from two manufacturers were used. The first specimen had a grain size of ASTM 7 to 8, and the second had a grain size of ASTM 6 to 7. Test samples were prepared by collapsing 1.5-mm-diam stainless steel tubing over a length of 0.5-mm-diam thermocouple material. The clamping of the collapsed tubing to the outside diameter of the thermocouple sample was intended to simulate the strong mechanical connection that exists between the FRS cladding and the internal thermocouples. The collapsed tubing was electrically heated through various thermal cycles, and the loop resistance of the thermocouples was monitored.

Those specimens with the smaller grain size (ASTM 7 to 8) were found to endure about 5000 cycles before

failure (open circuit and loss of electromotive force), or 2 to 3 times the number imposed on those with the larger grain size before failure. Also, prestraining the samples 5% prior to thermal cycling reduced their lifetime by a factor of 2.

Microstructures of most of the test samples showed void formation at the grain boundaries. Anderson attributed these voids to aluminum and chromium oxides that apparently formed at the respective grain boundaries and were removed by metallographic sample preparation. In both Anderson's investigations and investigations reported here, samples with voids were extremely brittle. The brittleness of Anderson's samples was attributed by Ludwig[8] to the brittle oxides that formed at the grain boundaries.

A quite different explanation of grain boundary voids has been offered by Dyson and Henn[9] and by Dyson and Rodgers.[10] In a study of a nickel-based alloy, they found that prestrain introduces microcracks that nucleate to form grain boundary voids when the material is subsequently heated above its recrystallization temperature. Further, the effect of stress is to enhance the formation of voids. Prestrain values of about 2% reduced the elongation-to-fracture measurements on samples by a factor of 2, indicating that even small values of prestrain result in grain boundary voids.

Although not specified, most thermocouples are received with a residual cold work of 1 to 3% (Ref. 1), presumably to adjust the Seebeck coefficient to meet the calibration curve. Further, as part of their assembly into an FRS, the thermocouples are strained an additional 0.5%. Thermocouples assembled into earlier, swaged FRSs were prestrained an additional 4 to 5% by the swaging process. Thus, the thermocouples in a swaged FRS (like those initially tested) have a prestrain of 5.5 to 8.5%, and those in a nonswaged FRS have a prestrain of 1.5 to 3.5%.

As the effects of prestrain were surfacing, the design of the CFTL FRS was evolving toward use of the nonswaged fabrication technique, which, by its nature, reduces thermocouple prestrain to a level below that at which large grain growth occurs (Fig. 4). A period of low-temperature operation at ~350°C for 1 to 2 d had also been incorporated as part of the operational sequence. After these changes were adopted, lifetime tests of thermocouples in nonswaged FRSs were extremely successful, although there was evidence of decalibration. Eight nonswaged FRSs with 27 type K thermocouples endured over 5,000 h of steady-state and transient testing, including over 36,000 thermal transient cycles. No thermocouples failed prior to FRS failure,

even though 4 rods endured 4,000 to 10,000 transient cycles, many as severe as 50°C/s.

Figure 5(a and b) compares photomicrographs of the Alumel thermoelement microstructure from a swaged FRS prototype with a nonswaged FRS prototype. Both FRSs endured about 1000 h of steady-state and transient operation and over 2000 thermal cycles. Sample 1 (Fig. 5a) failed after ~200 h of steady-state operation and 400 thermal cycles, while sample 2 (Fig. 5b) did not fail. Sample 1 was extremely brittle, but sample 2 was ductile even though the grains were relatively large.

Thus, while oxidation contributes to failure and should be minimized, the major cause of premature failure of small-diameter thermocouples appears to be prestrain-induced grain growth and grain boundary void growth or oxidation, causing reduced thermoelement cross-section and grain boundary embrittlement.

From the preceding discussion, the thermocouples apparently must have three characteristics if they are to endure high temperature and transient operation:

1. The thermocouples must be fully annealed when received. Any ensuing cold work occuring during their assembly should not exceed 1% and, for optimum results, should be removed prior to operating the thermocouples at or above their recrystallization temperature.
2. There must be a minimum of oxygen and moisture as well as hydroxides [such as $Mg(OH)_2$] or oxides (such as iron oxide) in the thermocouple insulation. This requirement will help to reduce the potential for oxidation of the chromium or aluminum in the thermoelements.
3. The final grain size of both thermoelement wires must be very small, with a recommended ASTM micrograin size 9 (~3970 grains/mm² or 0.016-mm average diameter).

Figure 4 shows that either very little or relatively large amounts of cold work are not detrimental to thermocouple grain size following recrystallization, while intermediate amounts can result in undesirable grain growth. A structure free of cold work (to prevent recrystallization during use) can be obtained by a recovery anneal below the material recrystallization temperature.[6] Therefore, the first characteristic mentioned previously can be obtained by specifying a recovery anneal as the last operation prior to thermocouple use.

The second characteristic can be obtained by specifying a 1000°C, <10-μ vacuum bakeout of the insulators

prior to their assembly into the thermocouple sheath, followed by assembly of the thermocouple bulk material in an inert atmosphere. The final characteristic results from optimization of the thermocouple fabrication process by careful annealing and by using large amounts of cold work to refine final grain size. The next sections discuss the background for and the methods used to accomplish this.

RECRYSTALLIZATION AND DRAWING

Recrystallization

Material recrystallization is a nucleation and growth phenomenon, the completion of which is dependent on annealing temperature, time, and cold work performed before annealing, as well as on composition variations. A schematic representation of the effect of prior cold work and initial grain size before cold working on the recrystallized grain size is shown in Fig. 4. The schematic suggests that a large amount of cold work is desired to refine grains by subsequent recrystallization; small amounts of cold work must be avoided unless they are too small to initiate recrystallization.

Because it is a nucleation and growth process, the amount of material transformed during recrystallization follows a sigmoidal distribution with time.[6] The time at temperature generally follows an Arhennius-type relationship with the material activation energy as the exponential variable.

If the grain size of two materials is to be minimized and if they must be annealed at the same temperature (as is the case with the Chromel-Alumel system in a thermocouple), then the amount of recrystallization of the material with the highest activation energy (Chromel) determines the annealing time. Thus the extent of recrystallization necessary for subsequent cold working of that material without fracture must be determined. This amount of recrystallization will determine the annealing time for the system and, therefore, the grain size of the material with the lowest activation energy (Alumel).

Drawing

Reference 11 provides an excellent review of drawing theory, part of which is presented here. The general equation for drawing is

$$\sigma_d = (1/\eta) \int \sigma \, d\varepsilon \, , \qquad (1)$$

where

σ_d = draw stress,
σ = material stress at ε,
η = process efficiency,
ε = true strain in drawing (cold work).

For materials that obey the strain-hardening power law,

$$\sigma = K\varepsilon^n \quad , \tag{2}$$

where K is a strength coefficient and n is the strain-hardening exponent. In this case, Eq. (1), after integration, becomes

$$\sigma_{d_1} = \sigma_{\varepsilon_1}\varepsilon_1/\eta(n + 1) \quad , \tag{3}$$

and for a second-draw pass, becomes

$$\sigma_{d_2} \cong 1/\eta \, \frac{\sigma_{\varepsilon_1} + \sigma_{\varepsilon_2}}{2} \, (\varepsilon_2 - \varepsilon_1) \quad , \tag{4}$$

where σ_ε is the flow stress of the material exiting the die, and

$$\varepsilon = \ln(A_0/A_1) \quad , \tag{5}$$

where A_0 and A_1 are the entering and exiting areas, respectively.

Figure 6 shows typical material stress and strain plots during steady-state drawing as described by Eq. (3). The material flow stress σ increases in accordance with Eq. (2) and is σ_ε at the die exit. The material is strained to $\varepsilon = \ln A_0/A_1$ at the die exit, and the draw stress σ_d acts on the reduced, strain-hardened material.

Figure 7 shows the drawing operation for a first draw described by Eq. (3) for $\eta < 1$ and $\eta = 1$ as well as Eq. (2) for the material. The material is influenced by the draw die as it passes through but is again in pure tension, in a work-hardened state, as it exits. It is normally work hardened enough so that it will neck and break if it yields. To prevent this, σ_d must be less than σ_ε so that the drawing limit is reached when $\sigma_d = \sigma_\varepsilon$. This is shown in Fig. 7 as the intersection between the σ_d and σ_ε curves. For this case Eq. (3) becomes

$$[\varepsilon_{max}]_{draw} = \eta(n + 1) \ . \qquad (6)$$

For pulling in pure tension,

$$[\varepsilon_{max}]_{pull} \approx n \ . \qquad (7)$$

Comparison of Eqs. (6) and (7) indicates that a maximum additional 100% elongation is possible with drawing as compared with pulling in pure tension. The amount achieved depends on η, the drawing efficiency. For a second drawing pass, the material flow curve would start at σ_ε, and, because the material is strain hardened, the σ_{d_2} curve would rise more sharply so that $(\varepsilon_2 - \varepsilon_1) < \varepsilon_1$.

The drawing efficiency η has been shown to depend only on the product of process frictional and redundant work terms and is given as[12]

$$1/\eta = f\Phi \ , \qquad (8)$$

where the process frictional work term is

$$f = (1 + \mu \cot \alpha) \qquad (9)$$

and the redundant work term is

$$\Phi = [1 + C(\Delta - 1)] \ , \qquad (10)$$

where

C = a constant (0.12 for wire),
μ = coefficient of friction,
α = draw die semiangle,
Δ = the deformation zone geometry factor $\cong \bar{d}/L$ (Fig. 6).

From Eqs. (8) through (10) the process efficiency depends only on Δ, μ, and α. To maximize the total cold work ε between anneals, the product of the factors containing α and Δ must be minimized. (The friction coefficient μ depends primarily on the lubricant. Many factors go into its selection and, although some investigations were conducted, to further minimize μ was beyond the scope of this work.)

Process parameters α and Δ are related by

$$\Delta = \frac{\pi}{180} \alpha \frac{(1 + e^{-\varepsilon/2})}{(1 - e^{-\varepsilon})} \ . \qquad (11)$$

The friction factor [Eq. (9)] asymptotically decreases with increasing α whereas the redundant factor [Eq. (10)] linearly increases with Δ so that their minima is reached at some intermediate value of α and corresponding Δ.

APPLICATION TO THERMOCOUPLE DRAWING – THE INTERNAL STRESS FACTOR

The preceeding analysis is adequate to arrive at optimum conditions for drawing of wire. For thermocouple drawing, however, drawability is normally limited by one of the internal thermoelements breaking (open circuiting). The drawing process must, therefore, be optimized based on the cold work and stresses occurring on these internal components. The friction factor [Eq. (9)] results from die-to-thermocouple surface forces; it should be independent of ε and can only influence the mean draw stress, not the radial stress distribution across the thermocouple.

The redundant term, however, has as its basis the occurrence of nonuniform die pressure and resultant internal stress and strain distributions as functions of the deformation zone geometry factor Δ. Figure 8 schematically represents stress and strain distributions as they might appear across a thermocouple cross section for $\Delta = 3$. The strain plot was extrapolated from hardness data[13] on lubricated wire for $\Delta = 6.9$ and lubricated strip for $\Delta = 4$, both with a true strain or cold work for $\varepsilon = 0.17$. From the plot, cold work can be seen to have a large variation across the cross section and is at a minimum internally. The average strain $\bar{\varepsilon}$ is increased above ε for the nonuniform distribution by the value of Φ given in Eq. (10). For $\Delta = 3$, the average cold work on the thermoelements is only about $0.8\ \varepsilon$ while the sheath incurs $\sim 2\ \varepsilon$. As Δ decreases towards one, the strain distribution becomes uniform. The implication is that low Δ drawing is more suitable to thermocouples if internal cold work is to be maximized as needed to refine thermoelement grain size.

The stress distribution of Fig. 8(c) further reinforces this notion. The distribution shown was derived from Hill's[14] slip-line field analysis (for frictionless plain-strain compression of a nonhardening material) and from Backofen's[15] *maximum* stress distribution analysis of Hill's data. Backofen showed that the variation in the internal stress distribution σ_{xx} from surface to center followed the same relationship with Δ as did the ratio of die pressure to surface yield stress ($\bar{P}/\sigma_y$) reported by Hill. The maximum in this internal stress variation is given by

$$\sigma_{xx\ max} = 2\ \sigma_y\ \lambda\ , \qquad (12)$$

where λ is the deformation zone slip-line apex angle and is 0 for $\Delta = 1$ and $0.43\ \pi$ for $\Delta = 8.75$. By interpolation, the maximum centerline to surface stress with Δ is then

$$\sigma_{xx\ max} = 0.35\ \sigma_y\ (\Delta - 1)\ . \qquad (13)$$

The stress distribution shown in Fig. 8(b) for $\Delta = 3$ is constant from the surface inward for a distance $L/2 \cong r_1/\Delta$ (where L is as shown in Fig. 6), then rises approximately linearly to a maximum of $\sim 0.7\ \sigma_y$ ($\sigma_y = 28 \times 10^6$ kg/m^2) at the center. The draw stress σ_d is $\approx 0.1\ \sigma_y$ larger because of this distribution, and the internal stress σ_{dE} is

$$\sigma_{dE} = \sigma_d + \sigma_\gamma = \sigma_d \gamma\ , \qquad (14)$$

where

$$\sigma_\gamma \cong 0.35\ \sigma_y\ (\Delta - 1) \left[1 - \frac{2}{3}\left(\frac{\Delta - 1}{\Delta}\right)^2\right] \qquad (15)$$

and the internal stress factor γ is

$$\gamma = 1 + \frac{\sigma_\gamma}{\sigma_d}\ . \qquad (16)$$

Equation (3) for the first draw in terms of the internal stresses now becomes

$$\sigma_{dE_1} \cong \Phi_1 f_1 \gamma_1 \frac{\sigma_{\varepsilon_1} \cdot \varepsilon_1}{n+1}\ . \qquad (17)$$

If there is to be a second draw of the same material, the stress distribution of the first draw must be taken into account. This distribution σ_{xx} is additive to the internal stress developed in the second draw. However, for $\Delta \leq 2$ on the first draw (which should normally be the case), $\overline{\sigma_{xx}} \ll \sigma_{xx}$ so that $\sigma_\gamma \cong \sigma_{xx}$ and the internal stress distribution can be accurately represented by σ_{γ_1}. A second distribution described by Eq. (15) is developed for the second draw, which results in σ_{γ_2}. The internal stress after the second draw is the sum of

these two stresses. Equation (4) for the second draw, in terms of the internal stress, becomes

$$\sigma_{dE_2} \cong \Phi_2 f_2 \gamma_2 \left(\frac{\sigma_{\varepsilon_1} + \sigma_{\varepsilon_2}}{2} \right) (\varepsilon_2 - \varepsilon_1) , \qquad (18)$$

where γ_2 is now

$$\gamma_2 = 1 + \left(\frac{\sigma_{\gamma_1} + \sigma_{\gamma_2}}{\sigma_{d_2}} \right) . \qquad (19)$$

Equations (3) and (4) for the draw stress and Eqs. (17) and (18) for the internal stress together enable complete modeling of the thermocouple drawing process. In their application to thermocouple drawing, the assumptions of nonstrain hardening and homogeneity must be recognized although the ability of the model to predict and improve the process will ultimately determine its usefulness. The strain-hardening assumption, although intended for nonstrain-hardening material, was shown by Backofen to still provide a reasonable upper-bound estimate of redundant strain properties of strain-hardening materials.[16] The effect of nonhomogeneity will be discussed in the next section.

To examine the internal stress as the limiting parameter in thermocouple drawing, the friction, redundant, and internal stress factors in Eqs. (17) and (18) must be calculated for various α and Δ. Figure 9 plots the $\Phi f \gamma$ product of Eq. (17) as a function of α for various amounts of cold work (ε). The deformation zone geometry factor Δ was determined for each α using Eq. (11). The draw stress σ_d was determined using Eq. (3), and K and n in Eq. (2) were determined to be 137.0 x 10^6 kg/m^2 and 0.28, respectively, from tensile tests of Inconel-sheathed, type K thermocouples.

The $\Phi f \gamma$ product acts as a multiplier to the useful work in drawing $\int \sigma d\varepsilon$, which results in the internal stress σ_{dE}. As the useful work increases (with ε) the efficiency $\eta_\varepsilon = 1/\Phi f \gamma$ improves. Figure 9 and Eq. (3) indicate that a first draw of $\varepsilon = 0.44$, with α between 10 and 12° and Δ between 1.6 and 1.9, is optimum and will give a σ_{dE}-to-σ_ε ratio of ~0.7, adequate to account for process and model uncertainties.

Additional cold work before annealing can be obtained with a second draw. However, as Fig. 10 shows, the cold work is less and process parameters are much more critical. The internal stress, resulting from redundant strain and characterized by Δ, dominates the

process for α above 3 or 4°, and friction dominates for α at less than 3°. The more pronounced minima and larger $\Phi f\gamma$ product for the second draw results from the greatly increased yield stress caused by strain hardening during the first draw. The yield stress, initially 35×10^6 kg/m², increases by a factor of 3 to 4 to σ_{ε_1} for the second draw. From Eq. (15), this proportionally increases the internal stress distribution with A. It is therefore extremely important to draw with A close to 1 on the second draw.

THERMOELEMENT GRAIN-SIZE REFINEMENT

The development to produce the refined-grain thermoelements was performed by ORNL during fabrication of a quantity of bulk thermocouple material for ORNL by Groth-Mazur, Inc., Addison, Illinois. Using the actual production equipment avoided the effects on the final results of small variations in specific parameters such as deformation, furnace temperatures, and temperature gradients.

The fabrication process consisted of the following steps. The magnesium oxide insulators were subjected to a 1000°C vacuum bakeout, and all materials were thoroughly cleaned. The thermoelement wires and magnesium oxide insulators were then assembled into an Inconel 600 sheath ~5 mm in diameter. The diameter of this assembly was reduced to 0.51 mm by a multiple-draw anneal cycle.

The development effort optimized both the drawing and the annealing processes to achieve the finest grain size possible, consistent with reasonable production times and material yields.

The new drawing and annealing schedule to obtain grain refinement was determined from (1) the preceding recrystallization and drawing theory, (2) literature information and physical property tests on the thermocouple components, and (3) industrial experience. The development consisted of three general tasks:

1. adjustment of annealing conditions to minimize grain growth of the Alumel thermoelement while still obtaining full recrystallization of the Inconel sheath and Chromel thermoelement,
2. definition of the existing drawing process in terms of Eqs. (3) and (4) and calculation of the friction factor f and coefficient of friction μ, and

3. determination of a new process to maximize the reduction between anneals by optimizing process parameters α and Δ in terms of Eqs. (17) and (18) and by comparison of draw and material stresses σ_{dE} and σ_{ε}.

Annealing conditions were determined by drawing annealed samples of Chromel and Alumel wire, and of assembled thermocouples, to 20 to 50% cold work, followed by annealing at several time-temperature conditions. Elongation-to-failure tests, as well as metallographic and microhardness examination of annealed samples, were then used. Optimum annealing conditions were found to be 1025°C for 60 s for a 1-mm-diam thermocouple. The annealing temperature was then held constant and the time varied to account for thermocouple mass-per-unit-length changes with diameter. Annealing times ranged from 120 s at about 3-mm diameter to 30 s at 0.5-mm diameter.

The applicability of drawing Eqs. (3) and (4) to a nonhomogeneous thermocouple was investigated by (1) conducting tensile tests on Inconel, Chromel, and Alumel wires and on type K, Inconel-sheathed thermocouples and (2) conducting draw tests on samples of thermocouples and the Chromel thermoelement. Figure 11 summarizes the tensile tests. Comparison of plots of measurements on the individual thermocouple components with the thermocouple measurements indicates that magnesium oxide insulation substantially affects the tensile characteristics of the thermocouple even though it cannot itself sustain a tensile stress.

Strain-hardening constants for Eq. (2) were obtained by curve fitting using the thermocouple and Chromel stress-strain plot, and these values were used in Eqs. (3) and (4). Draw stresses σ_{d_1} and σ_{d_2} were measured with a standard spring balance placed between the draw bench-puller jaws and the thermocouple or Chromel wire being drawn. The friction factor f was then calculated for each of the samples. The results showed f to be ~25% higher for thermocouple drawing than for wire drawing. This apparently reflects the work associated with movement of the insulation as the thermocouple is reduced as well as relative movement of insulation material and thermocouple metallic components as the insulation transmits the draw stress to the thermoelement during thermocouple reduction. The insulation thus contributes to the work of deformation without supporting a balancing tensile stress.

The increased friction factor for thermocouple drawing serves to increase the draw stress for a given reduction or, equivalently, to reduce the maximum elongation possible for a given draw stress.

Calculation of the coefficient of friction μ was accomplished by drawing thermocouple samples with existing dies (with $\alpha = 6°$) from $\varepsilon = 10\%$ to $\varepsilon = 30\%$ while measuring the draw stresses σ_{d_1} or σ_{d_2}. Strain-hardening constants from the thermocouple plot of Fig. 11 were used in Eqs. (3) and (4), and Eqs. (9) and (10) were used to calculate the frictional and redundant work terms, respectively.

Friction coefficient calculations from these measurements at first exhibited large variations. Draw dies that exhibited a larger-than-anticipated draw stress were replaced with new dies. In some cases, as much as a 40% decrease in draw stress was obtained for a new die under the exact drawing conditions imposed on the old one. This was attributed to die wear and variations in die bearing length B (Fig 6). After die replacements, μ was measured to be $0.19 \pm 10\%$ for 90% of the dies tested although variations up to 25% occurred.

The existing process consisted of drawing to 20 to 25% cold work in one step between anneals using draw dies with $\alpha = 6°$. During development, three new processes were obtained. In the first, the existing first-draw cold work (or slightly more) was retained, and a second draw of about 15% was added. Existing dies with $\alpha = 6°$ were used, in most cases, for both draws. In the second process, new dies with larger semiangles were designed, and the first-draw cold work was extended to about 42%. The final process combined the 40% maximum first-draw cold work with 15° second-draw cold work to obtain 55% cold work between anneals.

Optimization of the drawing and annealing schedule required continuity checks and elongation-to-failure tests of postannealed material. Excess stresses often did not immediately result in thermoelement open circuits. However, elongation-to-break tensile tests of postannealled thermocouples were excellent indicators of damaged or borderline material. Material correctly drawn and annealed experienced a true tensile elongation of 20 to 25% for both thermoelements and sheath, and the failure occurred initially in the sheath. Damaged material was characterized by initial failure of the Chromel thermoelement at a true strain of only 10 to 15% and, occasionally, failure of the Alumel thermoelement prior to that of the sheath as well. Material, once damaged, performed poorly in subsequent draws.

Table II summarizes part of the first process. As the table shows, the measured and calculated draw stresses for both first and second draws are in good agreement. However, internal stresses, calculated from Eqs. (17) and (18), are low on the first pass but high on the second pass. This is a direct result of the

high A values produced by using the existing dies with $\alpha = 6^{\circ}$. Open circuits of the Chromel thermoelement occurred on the second draw for σ_{dE}-to-σ_{ε} ratios of 108.4 and 99.8%. As development continued and the σ_{dE}-to-σ_{ε} ratio for the second draw was reduced by lowering α (and thus A), the incidence of open circuits decreased. All failures were caused by Chromel thermoelement opens; no sheath breaks occurred.

Table III summarizes the second and third draw-anneal processes. The second process used draw dies with a semiangle of 11°, based on the predictions of Fig. 9, and an attempt was made to limit die-bearing length to 15% of L (Fig. 6). Correlations between measured and calculated draw stresses decreased considerably with an additional 10 to 15% first-draw cold work. First-draw predicted values average 17% below those measured. Extrapolation of the strain-hardening constants to high cold work values or frictional behavior that results in the friction factor f increasing with cold work [Eq. (9)] could account for this.

Process III, presented in Table III, summarizes the latest draw-anneal schedule, still under development, in which 55% cold work between anneals is achieved by drawing in two draws. Dies for the second-draw pass were designed with $\alpha = 3^{\circ}$ in accordance with the predictions of Fig. 10. The measured first-draw stresses were also higher than those predicted by Eq. (3), but the measured second-draw stresses were lower in contrast to those of process I with lower first-draw cold work.

Errors in the strain-hardening constant n, the redundant work term Φ, or the friction factor f at high first-draw cold work must have occurred to account for these discrepancies. Second-draw redundant work is high for process I and low for process III, so higher redundant errors would be expected in process I than in III if Φ errors dominate. Some strain-hardening error at high cold work is probable. However, draw tests at $\varepsilon \cong 0.42$ that resulted in sheath breakage ($\sigma_{\varepsilon} = \sigma_{d_1}$) indicated that σ_{ε} is within about $\pm 8\%$ of the value obtained from thermocouple strain-hardening constants. Since the apparent coefficient of friction μ is higher for thermocouple drawing than for wire drawing, it is reasonable to assume that an additional increase in μ at high cold work accounts for much of the discrepancy in calculated vs measured draw stress. For this assumption to be true, μ, which is constant at 0.19 for cold work up to 30%, must increase sharply to $\mu \cong 0.3$ for cold work above 40%. No mechanism is yet available to account for this phenomena.

The schedule developed in phase I was used to produce thermocouple bulk material with an average length of about 50 m. Failure of the Chromel thermoelement caused by high internal stresses was the limiting factor. The phase II schedule was used to produce thermocouple bulk material with an average length of about 100 m with sheath breakage limiting the process. Although long bulk material lengths are possible with process III above about 1-mm diameter, development has not been completed to obtain 0.5-mm material in lengths comparable with those of process II.

First-draw cold work for both processes II and III is limited to a maximum of about 42% by sheath breakage. The process III second draw, while extending the cold work up to 20%, is limited on the low side of a by friction and on the high side by high internal stresses. When two draws are used to obtain maximum cold work, diametrical tolerances of both draw dies are critical to maintaining second-draw cold work within 10 to 20% as thermocouple diameter is reduced below about 1.5 mm.

More than 3500 m of bulk thermocouple material was produced during process development. Figure 12 shows the microstructure of the Chromel and Alumel thermoelements resulting from an average of 40% cold work between anneals. The micrograin sizes of the thermoelements are ASTM 11 and 9 (15,900 and 3,970 grains/mm^2), respectively.

SUMMARY AND CONCLUSIONS

Premature failure of small-diameter, type K Inconel-sheathed thermocouples required an investigation into the causes of failure and ways to improve lifetime. Failure was judged to be caused by thermoelement grain growth and embrittlement. The brittle condition was characterized by large grains with respect to thermoelement diameter and by voids and oxides formed along the grain boundaries. Major contributors to this condition were impurities introduced during thermocouple assembly and, particularly, critical amounts of cold work left in the thermocouple because of incomplete annealing or introduced by swaging during FRS fabrication. The embrittled thermocouples subsequently failed when thermally activated expansion mismatched between them, and the FRS cladding imposed relatively small axial strains on the thermoelements, causing grain-boundary separations. Three characteristics were established as important to improved thermocouple performance under high-temperature, thermal cycling conditions:

1. elimination of prestrain in the thermoelements prior to operation of the thermocouple above their recrystallization temperature;
2. minimization of oxygen, moisture, and hydroxides within the thermocouple; and
3. refinement of the thermoelement grain size to meet ASTM micrograin size 9 or smaller (as a goal).

Significant improvements in thermocouple performance were demonstrated simply by eliminating small amounts of cold work in the material by a recovery anneal prior to their use. Additionally, a 1000°C $\leq$ 10 μ bakeout of the insulators prior to their assembly into the thermoelement sheath, careful cleaning, and thermocouple assembly with an inert cover gas were added to the thermocouple fabrication process. Finally, refinement of thermoelement grain size to ASTM micrograin size 9 for Alumel and 11 for Chromel was accomplished by development of a new draw-anneal process.

Annealing conditions were established as 1025°C for 30 to 120 s depending on thermocouple diameter. The drawing process was optimized by application of the general wire-drawing equation $\sigma_d = f\Phi\int\sigma d\varepsilon$ to thermocouple drawing. The equation was extended to describe internal stresses for multiple-pass drawing of thermocouples, and process parameters were evaluated and optimized to increase cold work between anneals from 25 to 60%. This maximum cold work level was achieved in two draws between anneals averaging 40 and 15%, respectively. High second-draw yield stress caused by first-draw strain hardening combined with frictional losses to limit second-draw cold work to 10 to 20% with a draw die semiangle of 3 to 4°. The friction factor $f = (1 + \mu \cot \alpha)$ was found to be about 25% higher for thermocouple drawing than for equivalent wire drawing. It also appeared to be a function of the per-draw cold work level when cold work was >30%.

Improved grain size was most easily achieved by single-pass drawing to an average of 40% cold work between anneals. Although further improvement in grain size occurred with the 55%, multiple-pass process, diametrical tolerances were critical below about 1.5 mm because small diametrical changes in either draw die caused a relatively large second-draw cold work change.

Table 1. FRS thermocouple requirements

Type	K (Chromel-Alumel)
Sheath	Inconel 600
Insulation	MgO
Junction	Insulated
Length, mm	1550 to 2750
Diameter, mm	0.51
Lifetime, h	1000 minimum
Time at 1100°C, h	40
Time above 1100°C, min	~10
Thermal cycles	2000 minimum
Cycling range, (°C)	
Normal	300 to 800
<10 cycles	300 to 1400
Ramp rate, °C/s	1 to 50
Accuracy, °C	±8 to 800
	±15 from 800 to 1400

Table II. Type K, Inconel-sheathed thermocouple draw-anneal schedule – process I

Percent cold work (ε)		Anneal s at 1025°C	Calculated draw stress σ_d (kg/m²)	Measured draw stress σ_d (kg/m²)	Error (%)	Calculated internal stress σ_{dE} (kg/m²)	$\sigma_{dE}/\sigma_\varepsilon$ x 100 (%)	Process parameters	
per draw	total							α	Λ
26.4			58.6	59.3	-1.2	66.0	69.9	6	1.6
15.3	41.7	90	52.7	51.9	+0.6	100.1	93.3	6	2.7
30.5			68.9	69.5	+0.6	74.1	75.4	6	1.4
12.2	42.7	60	45.5	45.7	-0.2	104.3	96.6	6	3.4
28.1			62.8	60.9	+3.1	66.5	69.3	6	1.5
9.7	37.8	45	40.4	50.8	-20.5	113.1	108.4	5	3.6
27.6			61.4	61.6	-0.3	67.2	70.3	6	1.5
12.5	40.1	45	45.6	47.8	-2.5	105.9	99.8	6	3.4
28.6			64.2	64.6	0.6	70.2	72.7	6	1.5
11.5	40.1	30	50.6	46.7	+8.4	89.0	83.9	4	2.4

Table III. Type K, Inconel-sheathed thermocouple draw-anneal schedule – processes II and III

Percent cold work (ε)		Anneal s at 1025°C	Calculated draw stress σ_d (kg/m²)	Measured draw stress σ_d (kg/m²)	Error (%)	Calculated internal draw stress σ_{dE} (kg/m²)	$\sigma_{dE}/\sigma_\varepsilon$ x 100 (%)	Process parameters	
per draw	total							α	Δ
				Phase II					
40.8		90	74.4	84.7	-12.2	94.2	88.4	11	1.9
40.8		60	74.4	82.8	-10.1	92.3	77.7	11	1.9
37.8		45	68.2	86.4	-21.1	96.6	92.6	11	2.0
39.3		45	71.7	87.3	-17.9	97.5	92.4	11	2.0
41.8		30	76.0	99.6	-23.7	108.0	100.5	11	1.8
				Phase III					
41.5			76.1	89.9	-15.4	99.4	92.8	11	1.9
15.9	57.4	60	85.5	70.5	+21.3	90.7	77.3	3	1.3
42.5			77.6	101.7	-23.7	110.1	102.1	11	1.8
18.6	61.1	45	98.9	90.0	+9.9	101.6	85.1	3	1.1
43.4			79.7	110.6	-27.9	119.0	109.7	11	1.8
17.8	61.2	30	96.0	92.1	+4.2	108.1	90.5	3	1.2

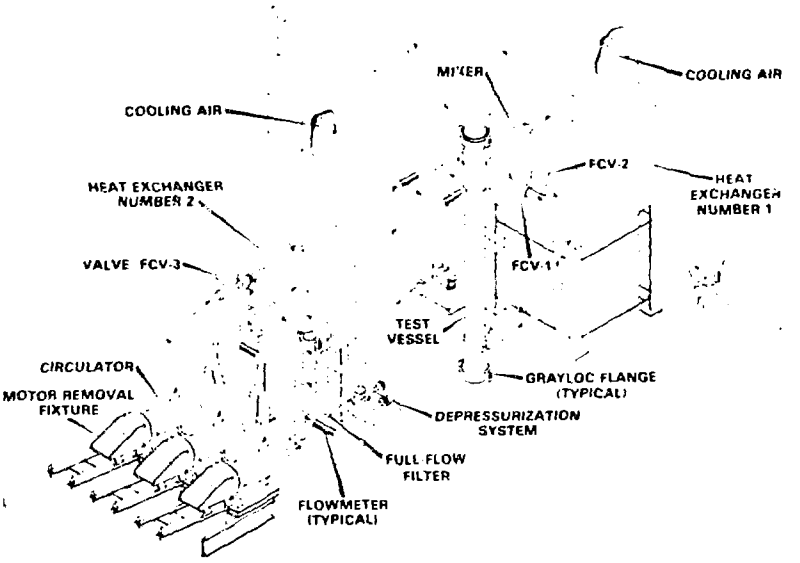

Fig. 1. Core flow test loop.

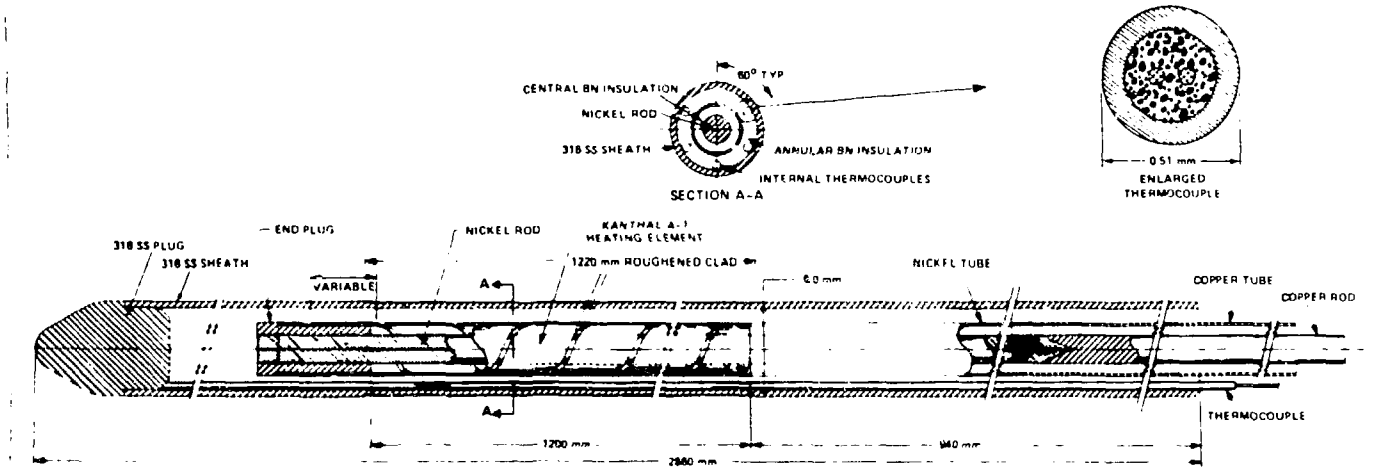

Fig. 2. GCFR-CFTL FRS.

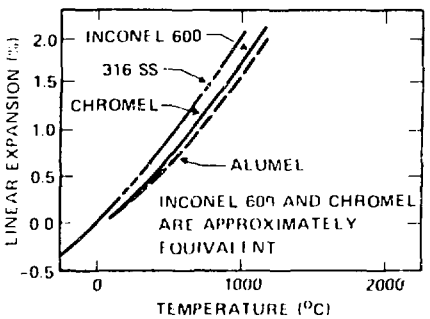

Fig. 3. Average linear thermal expansion of materials for CFTL FRS cladding and thermocouple components.

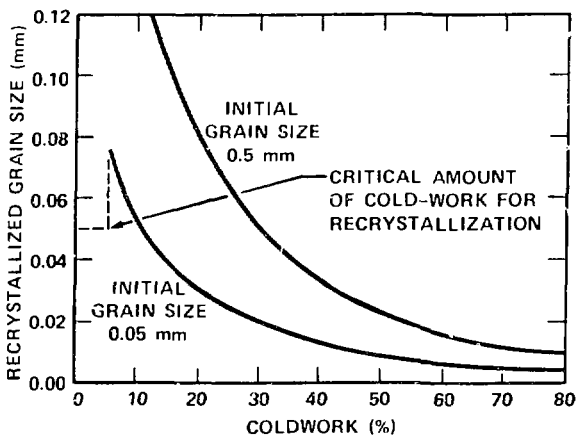

Fig. 4. Schematic curves of recrystallized grain size vs amount of cold work before recrystallization.

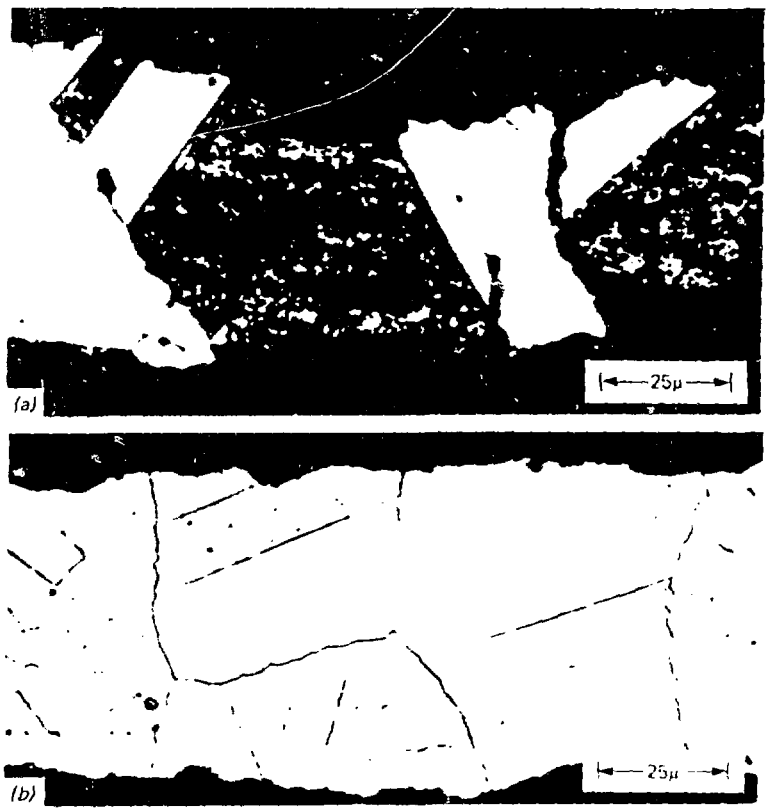

Fig. 5. Photomicrographs of Alumel thermoelement from (a) a swaged FRS and (b) a nonswaged FRS, both of which endured ~1000 h of operation with more than 2000 thermal cycles. Voids in (a) render it very brittle while the void-free sample of (b) is ductile (original reduced 8%).

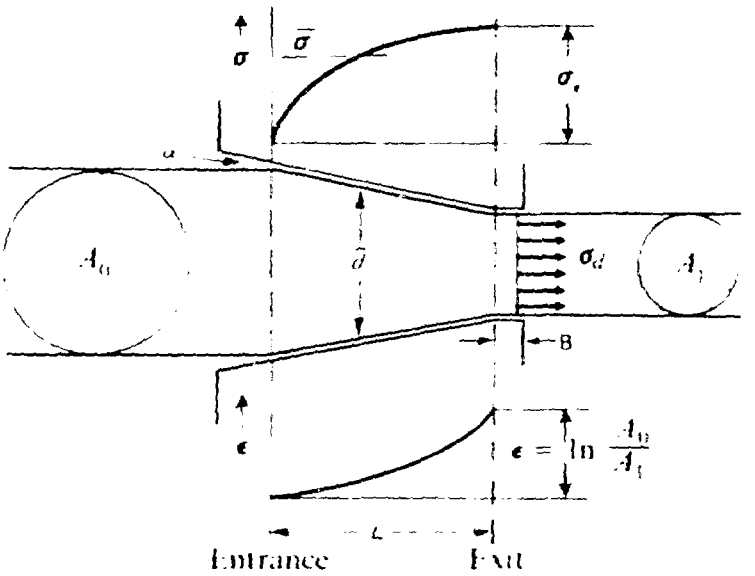

Fig. 6. The steady-state drawing operation.

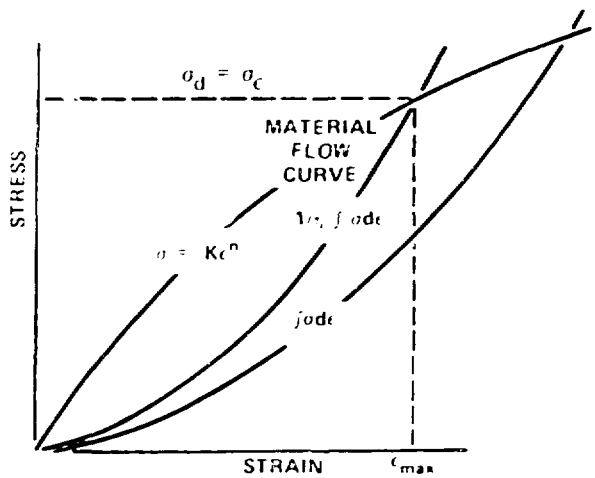

Fig. 7. Flow-curve ($K\varepsilon^n$) for a solid wire that exhibits strain hardening as well as work curve for ideal ($\int \sigma d\varepsilon$) and typical ($1/\eta \int \sigma d\varepsilon$) drawing process.

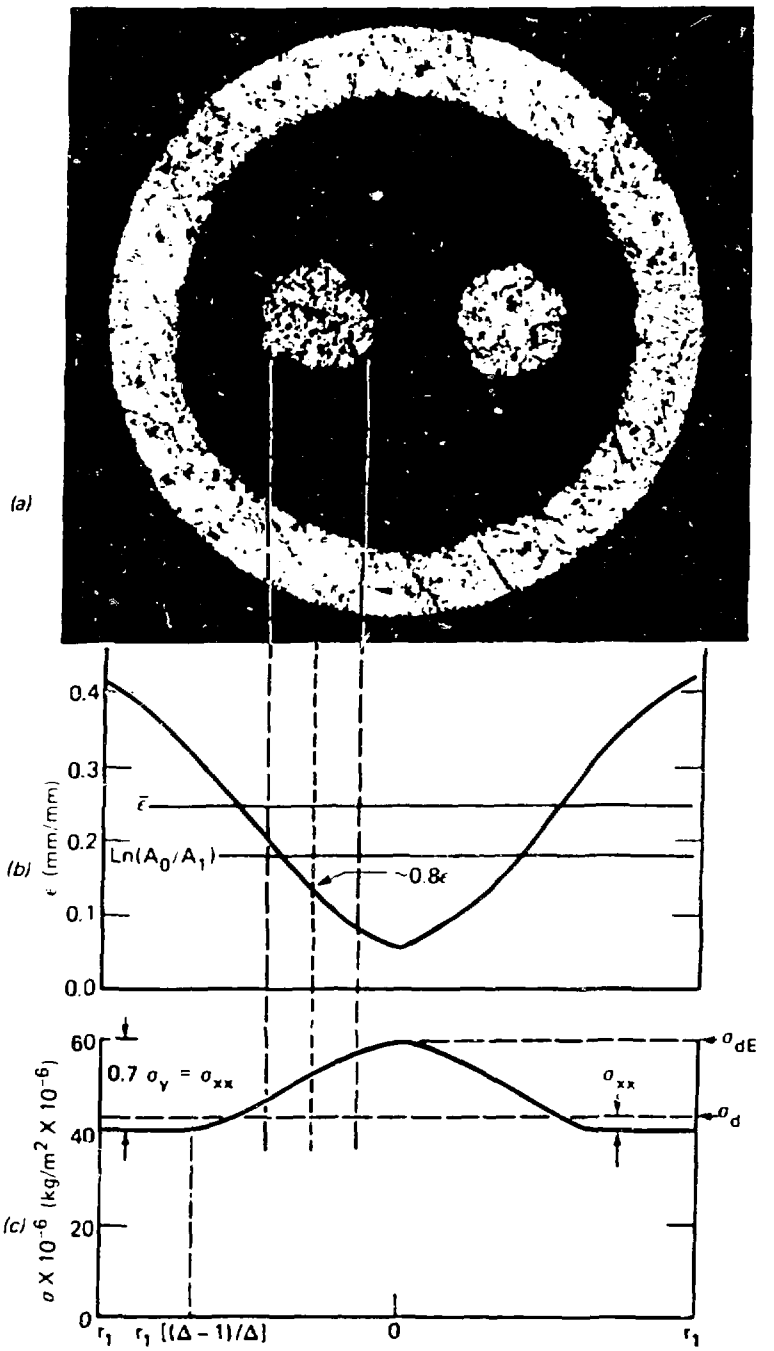

Fig. 8. A schematic representation of radial stress and strain pattern across a thermocouple drawn with $\Delta = 3$ and $\epsilon = 0.17$. Average strain is increased to $\bar{\epsilon}$ by nonuniform distribution, and strain of thermoelement is about 0.8ϵ. Internal stress is maximum in the center and depends on yield stress as well as Δ.

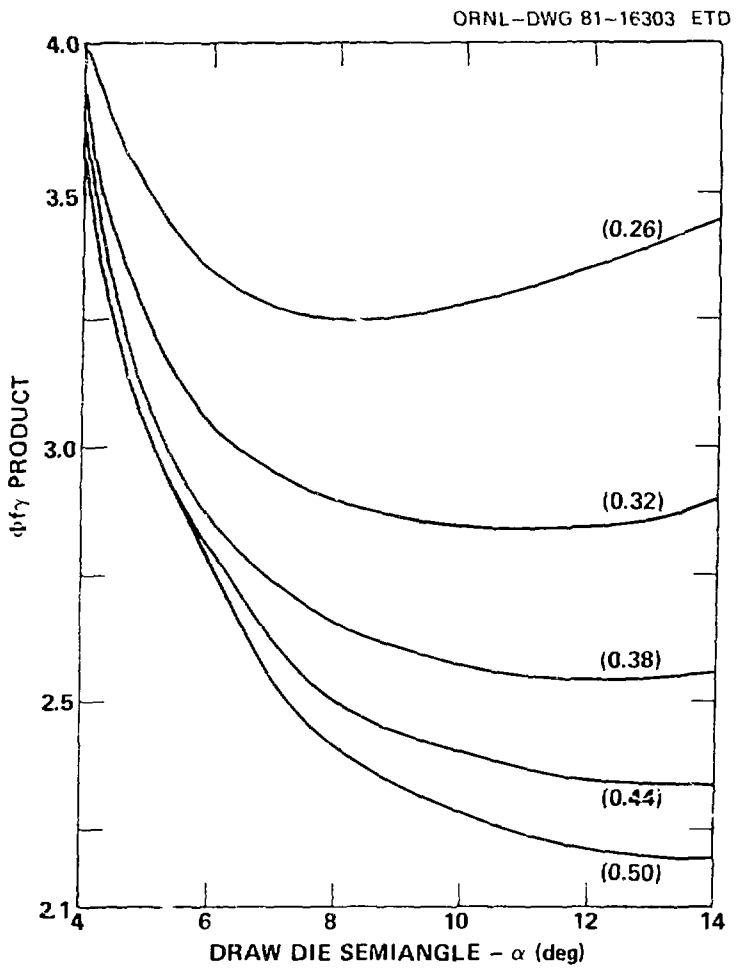

Fig. 9. $\phi f\gamma$ product vs draw-die semiangle at various amounts of cold work (μ = 0.19).

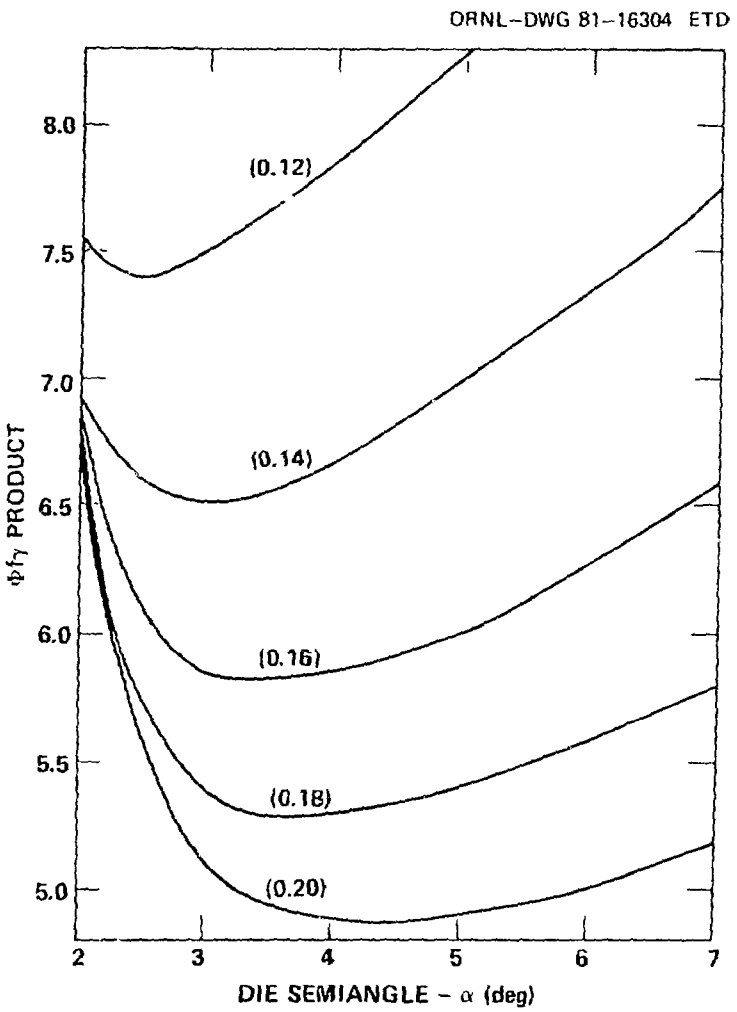

Fig. 10. $\Phi f\gamma$ product vs draw-die semiangle for various amounts of second-draw cold work (μ = 0.19).

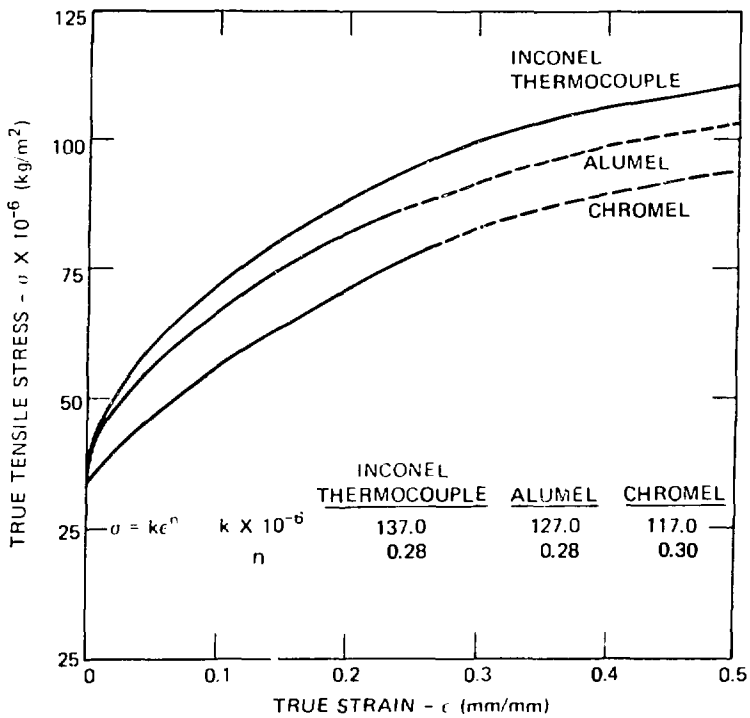

Fig. 11. True stress vs true strain for an Inconel-sheathed Type K thermocouple and for Chromel and Alumel thermoelements.

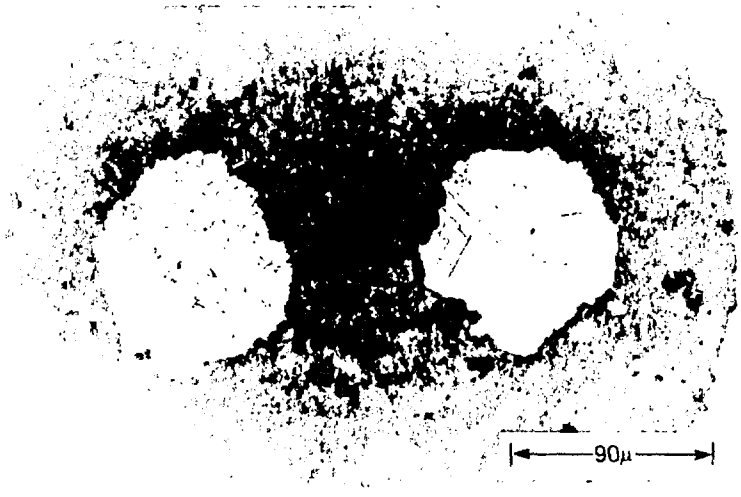

Fig. 12. Chromel (left) and Alumel average grain size is 9 and 17 μ (ASTM 11 and 9), respectively, after grain size refinement (400x). (Original reduced 16%).

REFERENCES

[a]Research sponsored by the Office of Research and Technology, U.S. Department of Energy under contract W-74050-eng-26 with the Union Carbide Corporation-Nuclear Division.

[b]Permanent address: Oak Ridge National Laboratory, P.O. Box X, Oak Ridge, Tennessee 37830.

[c]Permanent address: Y-12 Development Division, P.O. Box Y, Oak Ridge, Tennessee 37830.

1. Potts, J. F., Jr., and McElroy, D. L., *Thermocouple Research to 1000°C — Final Report November 1, 1957 through June 30, 1959*, ORNL-2773, Oak Ridge National Laboratory, 1969.

2. Anderson, R. L., and Kollie, T. G., *Accuracy of Small Diameter Sheathed Thermocouples for the Core Flow Test Loop*, ORNL-5401, Oak Ridge National Laboratory, 1979.

3. Reed-Hill, R. E., *Physical Metallurgy Principles*, Van Nostrand Reinhold Company, 1964, p. 144.

4. Gat, Uri, and Kasten, P. R., *Gas-Cooled Reactor Program's Annual Progress Report for Period Ending December 31, 1978*, ORNL-5560, Oak Ridge National Laboratory, p. 150.

5. Spooner, N. F., and Thomas, J. M., "Longer Life for Chromel-Alumel Thermocouples," *Met. Prog.* (November 1955).

6. Shewman, P. G., *Transformations in Metals*, McGraw-Hill Book Company, New York, 1969, Chap. 3, pp. 69–125.

7. Gat, Uri, and Kasten, P. R., *Gas-Cooled Reactor Programs Annual Progress Report for Period Ending December 31, 1978*, ORNL-5560, Oak Ridge National Laboratory, pp. 140–62.

8. Ludwig, R. L., private communication to Anderson, R. L., Jan. 15, 1979; Subject: Examination of Thermal Cycled Type K Sheathed Thermocouples.

9. Dyson, B. F., and Henn, D. E., "The Effect of Room Temperature Prestrain on Grain Boundary Cavitation in Nimonic 80A," *J. Micros.*, 97 (1/2), 165–70 (January–March 1973).

10. Dyson, B. F., and Rogers, M. J., "Prestrain, Cavitation, and Creep Ductility," *Met. Sci. J.* 8, 261–66 (1974).

11. Backofen, W. A., *Deformation Processing*, Addison-Wesley Publishing Co., Inc., Reading, Mass., 1972, pp. 190–196.

12. Backofen, W. A., *Deformation Processing*, Addison-Wesley Publishing Co., Inc., Reading, Mass., 1972, pp. 227–228.

13. Backofen, W. A., *Deformation Processing*, Addison-Wesley Publishing Co., Inc., Reading, Mass., 1972, pp. 138–139.

14. Hill, R., *The Mathematical Theory of Plasticity*, Oxford University Press, Amon House, London, England, 1964, p. 257.

15. Backofen, W. A., *Deformation Processing*, Addison-Wesley Publishing Co., Inc., Reading, Mass., 1972, pp. 145–147.

16. Backofen, W. A., *Deformation Processing*, Addison-Wesley Publishing Co., Inc., Reading, Mass., 1972, p. 140.